RECENT CHANGES IN THE CLIMATE AT THE DEAD SEA – A PRELIMINARY STUDY

P. ALPERT * and H. SHAFIR
Department of Geophysics and Planetary Sciences, Tel-Aviv University, Israel 69978
D. ISSAHARY
Dead Sea Works, Research Department, South Dead Sea, Israel

Abstract. In the last decade pan evaporation measured at the Southern Dead Sea has significantly increased. Wind, temperature and humidity measurements at the Dead Sea starting in the 1930s as well as 3-D model simulations all seem to indicate a statistically significant change in the local climate of the Dead Sea region. The potential contribution to this climatic change through the weakening of the local land-sea breeze circulation caused by the reduction in the Dead Sea surface area in 1979–1981, is examined. It is suggested that since the breeze tempers the Dead Sea climate, its weakening has caused the air temperature to increase, the relative humidity to decrease and thus increased the pan evaporation. The climatic changes as implied by the MM4 Mesoscale PSU/NCAR model simulations, seem to fit the observed changes and to suggest a local tendency to the more arid climate that now prevails to the south of the study region.

1. Introduction

The Dead Sea has attracted attention from ancient times as it does today; it is located at the lowest spot on the earth; currently, about –410 m below sea level. It is a part of the Rift Valley, extending from the Taurus mountains in Turkey to East Africa. Its waters are the densest and saltiest of any natural water body, and gave the Dead Sea its name, as almost no form of life higher than bacteria exists in this water, see Oren (1993). The potash factory, located on the southern part of the lake, makes use of the concentrated salts and the arid climate to manufacture potash, bromine and other salts by natural evaporation. The arid climate provides high values of evaporation which make the production process successful.

It is this special Dead Sea climate which is the focus of this paper. The pioneering studies of the Dead Sea climate were those of Ashbel, who made extensive measurements of meteorological as well as hydrological parameters starting in the 1930s; these were summarised in Ashbel (1975). In recent years, Bitan (1974) has investigated special features of the Dead Sea wind regimes.

Recently, Israel and Jordan have made extensive use of the water previously flowing into the Dead Sea. As a result, parts of the Dead Sea have dried. Steinhorn (1981), Klein (1982), Anati and Shasha (1989) and others investigated these changes in the area of the Dead Sea from different points of view. One result has been the separation of the Northern basin of the Dead Sea

from the Southern basin which only continues to exist artificially as a water surface with a depth of only 1–2 m, and is used as an evaporation pond for the

* Work partly done while on Sabbatical Leave at Data Assimilation Office, Code 910.3, NASA/GSFC, Greenbelt, MD20771.

Climatic Change **37:** 513–537, 1997.

local mineral industries (Klein, 1985). The position of the region studies is shown in Figures 1 and 2.

The fact that the Dead Sea influences the climate of its neighboring regions was discussed by Ashbel (1939). More recently Bitan (1977) investigated these influences on the local wind regime. In the last decade evidence has emerged that the drying of the Dead Sea has caused a change in the climate of the Dead Sea basin. Stanhill (1994) calculated the effect of the Sea's increasing salinity and temperature in reducing the lake evaporation. Cohen and Stanhill (1996) have shown that the solar irradiance and maximum temperature to the South Dead Sea have decreased, and the minimum temperature increased during the last 50 years.

In this paper, the climatic change at the Dead Sea caused by the drying of the Dead Sea is investigated. The recent rapid increase of the pan evaporation in Sdom (S in the figures) is described in Section 2. Section 3 suggests that the drying of the lake may explain the recent local change in the Dead Sea climate. Section 4 discusses the significance of the variations in the lake breeze to the Dead Sea climate change. Three-dimensional numerical modeling (PSU/NCAR version MM4) is described in Section 5. The model was run with the extended area of the Dead Sea in the past as well as with its present reduced area. Model results agree with the evidence presented that a climate change has occurred in the Dead Sea.

2. The Change of Evaporation Climate to the South Dead Sea

2.1. THE PRESENT STATE OF THE DEAD SEA

The general region of study is presented in Figure 1, while the Dead Sea region and measurement stations are shown in Figure 2. Part of the former Dead Sea seen in Figure 2 has dried; and the former Lisan Straits west of the former Lisan peninsula is now dry land. The Northern basin is thus completely disconnected from the Southern basin, which exists as an artificial lake, with water pumped from the Northern basin via a canal to the Southern basin to maintain a depth of not more than 1–2 m (Klein, 1985). The local industries use the Southern basin as evaporation ponds.

2.2. PAN EVAPORATION CHANGES IN SOUTH DEAD SEA

In recent years pan evaporation measured at Sdom ($31^\circ 02'$ N, $35^\circ 24'$ E, see station denoted by S in Figure 2) have shown a 12–15% increase (Figure 3). The pan is a standard U.S. Class A pan, 1.2 m diameter, depth of 25 cm. It is located within the evaporation ponds region and inside a fenced area of the Dead Sea Works, and is protected to avoid animal or bird interference. The measurements are performed as follows. Each day at 8 a.m. three micrometer readings of the pan level are taken and the average reading is recorded. Evaporation from the pan is corrected to include the small amounts of rainfall.

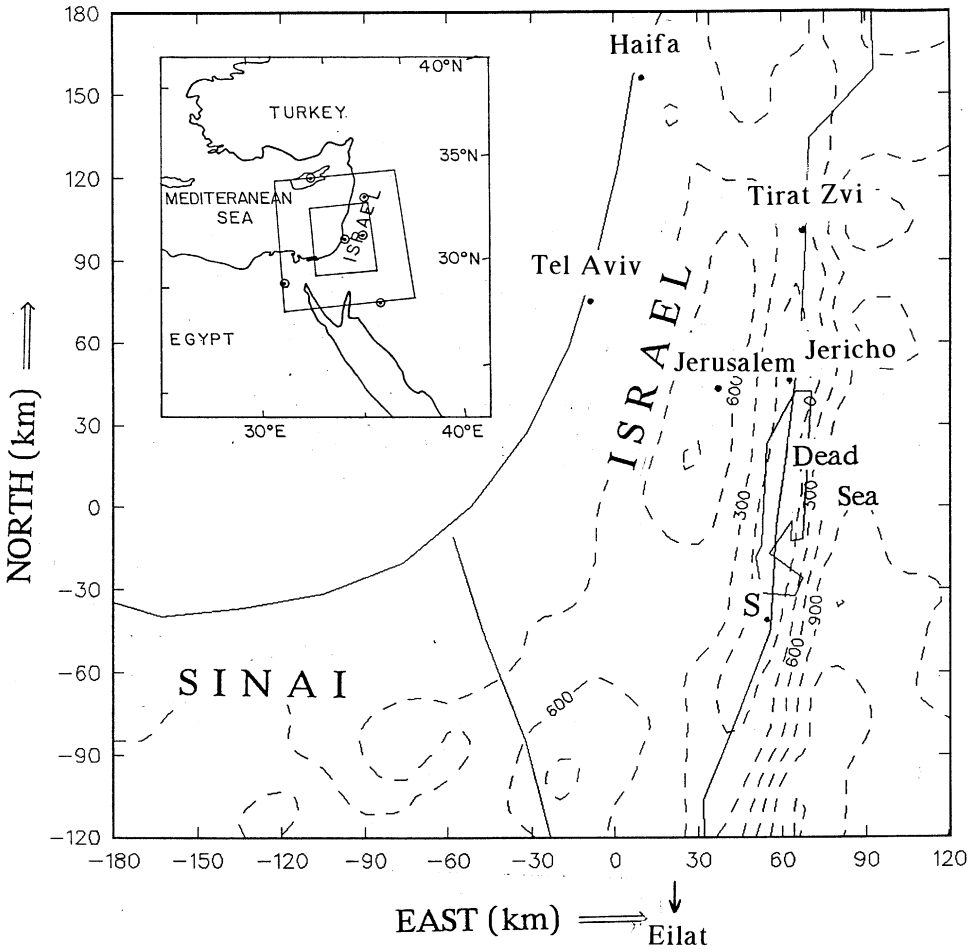

Figure 1. Area of the study domain. Topography contours are dashed with 300 m interval. At the north westerly corner the general area (East Mediterranean) is shown along with the extended model domain with the six radiosonde locations employed in the model simulations.

Comparison of two pan measurements performed in parallel for several years in Sdom indicates the measurements to have a variance of 2.6 $mm^2\ d^{-2}$ and a standard deviation of about 1.6 mm d^{-1}. Since the variance is additive, the annual standard deviation was estimated as 30.6 mm yr^{-1}, less than 1% error in the annual values in Sdom.

In the 1960–1980 period, the annual totals of pan evaporation values were 3.40–3.60 m yr^{-1}. In the last decade it increased to 3.80–4.00 m yr^{-1}, and in 1994 it reached

a value above 4.00 m yr^{-1}. Since 1981 values below 3.50 m yr^{-1} have not been recorded, while in earlier periods about half of the years exceeded this value; see Figure 3.

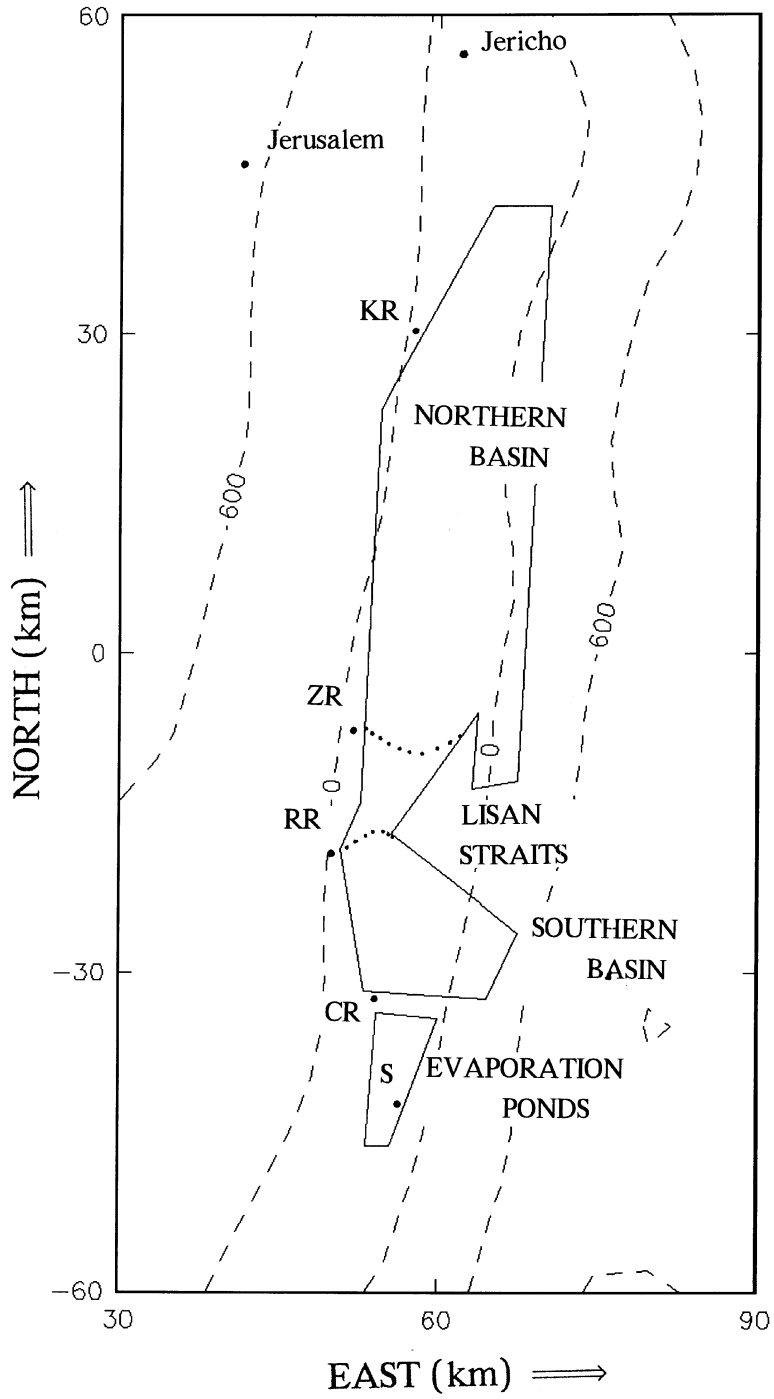

Figure 2. Study domain of the Dead Sea. Topography contours are with 600 m interval. The area between the dotted lines is the drying zone. Letters KR, ZR, RR, CR and S stand for locations of Kidron River, Zeelim River, Rachaf River, Chemar River and Sdom, respectively.

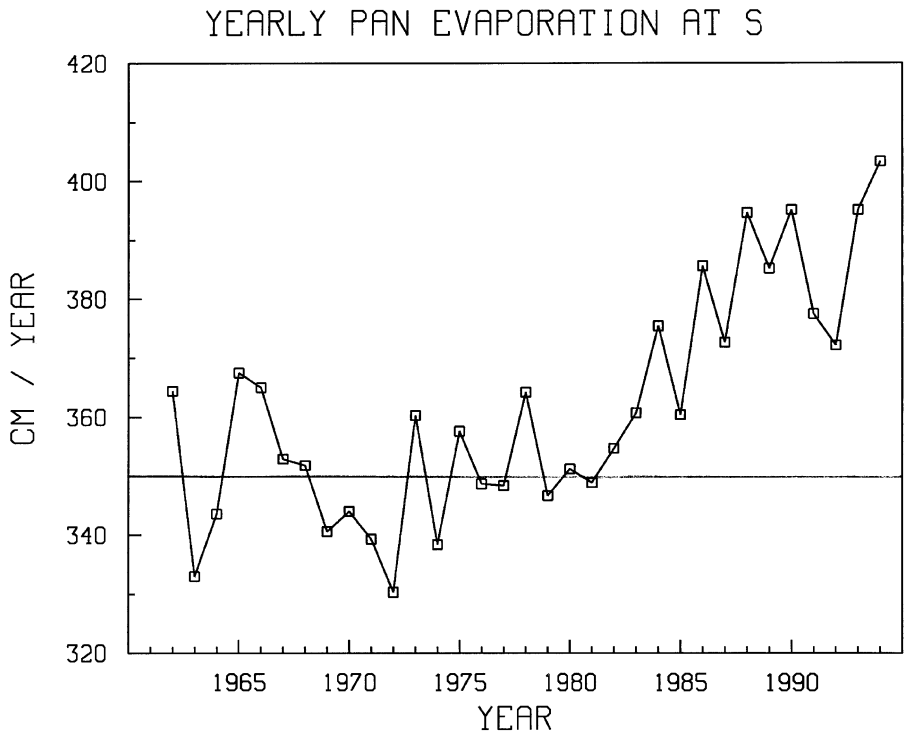

Figure 3. Annual pan evaporation at Sdom (S) for the years 1962–1994. Line of 350 cm yr^{-1}, was added.

The purpose of this paper is to explore the reasons for this increase. Two years with relatively low evaporation can be related to volcanic eruptions. The Agung eruption in March 1963 was a major one with a Dust Veil Index of 800 (Mass and Portman, 1989), and in this year a sharp decline in the evaporation was recorded at S (Figure 3). The Pinatubo eruption in June 1991 was also major (Song et al., 1996), and an evaporation decline was recorded in 1991 and also in 1992. 1992 was also a year with heavy precipitation that may partly explain the evaporation reduction in that year. For instance, in Jerusalem an exceptionally high rainfall of 1134 mm yr^{-1} was reported for 1992 as compared to the 30 y normal of 492 mm yr^{-1} (Israel Met. Serv., 1967).

The annual rainfall at Sdom is only 50 mm yr^{-1} and its effect on evaporation is in general small. Correlations between Sdom evaporation and Sdom or Jerusalem rainfall values for the period 1960/1–1994/5 were calculated and found, as expected, negative but very low*, i.e., –0.11 and –0.08 respectively. Similarly, Cohen

* The *indirect* effect of rainfall on the evaporation through the change of the Dead Sea area and the local climate is apparently much stronger and is the main issue of the present study. Obviously, this indirect relation of rainfall-evaporation involves other factors as well such as rainfall on the catchment area, river flow and water usage.

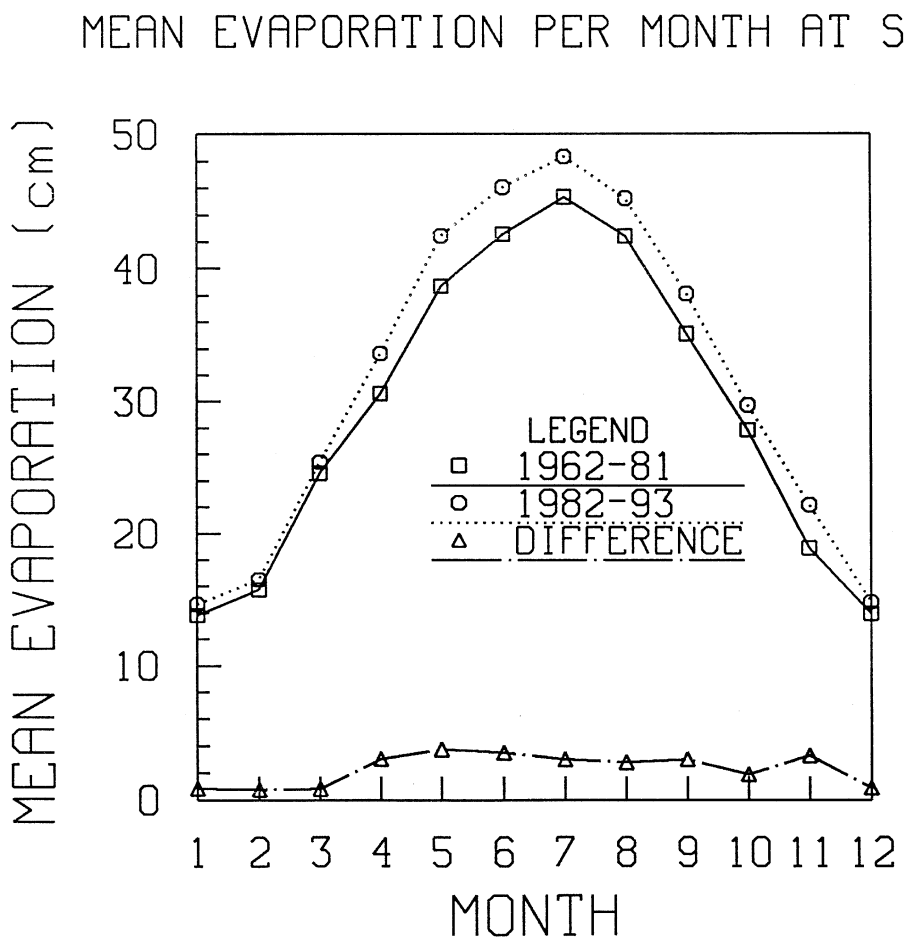

Figure 4. Average monthly evaporation at Sdom (S). Current period (1982–1993) compared with previous period (1962–1981), and the monthly difference between the two periods.

and Stanhill (1996) have recently analyzed the variance explained by the rainfall influence over the annual maximum temperature variability employing a multiple linear regression analysis in Sdom. They found that rainfall explains only 6% as compared to 30% in other Jordan Valley locations in the North. They have also found negative relationships in all cases, i.e., temperature decreased with increased rainfall.

Figure 4 presents mean pan evaporation per month in recent years (1982–1993), as compared to earlier years (1962–1981). The differences in the monthly values can also be seen at the bottom of the figure. The main increase is found in the Spring–early Summer months with a peak in May, while the winter contribution to the change is insignificant.

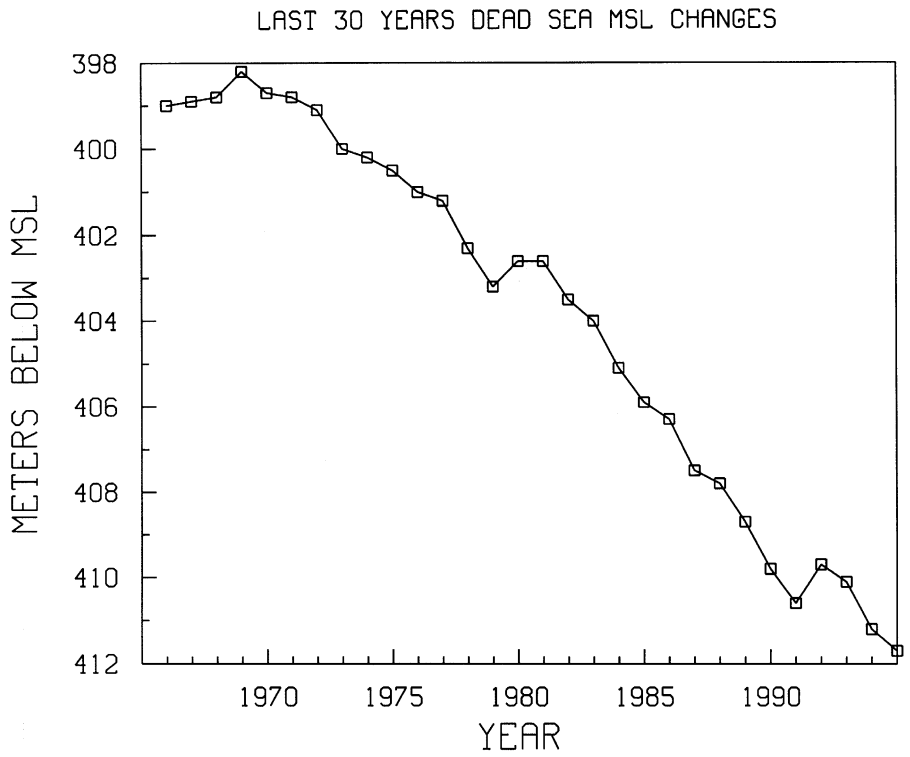

Figure 5. Dead Sea MSL changes for 1966–1995 following Anati et al. (1987), Anati and Shasha (1989) and Anati (1997).

3. Local Dead Sea Climatic Change as Affected by the Drying Up of the Sea?

3.1. DRYING OF THE DEAD SEA

Figure 5 shows the recent changes in the mean sea level of the Dead Sea. According to Anati and Shasha (1989) the average rate of the drop in the level of the Dead Sea was –0.8 m yr^{-1} during 1981–1989. In 1969–1977, the average drop was less than half –0.39 m yr^{-1}. The rapid drop of the Dead Sea MSL was associated with a sharp decline in the Dead Sea surface area. The Dead Sea area was nearly constant at 940–950 km^2 during 1940–1950 (Stanhill, 1994). In 1977–1979, when the MSL was –402 m, the Northern basin became disconnected from the Southern basin and about 50 km^2 west to the Lisan Straits have dried out during a short period of time. In 1981, the area was only 796 km^2 (Steinhorn, 1981), and the remaining Southern basin has a depth of only 1–2 m. It is interesting to note that the pan evaporation increase at Sdom began in 1981 following the major contraction of the Dead Sea. During 1980–1990, areas of the Northern basin dried, and the Dead Sea area in 1987 was 686 km^2 (*Hydrological Year Book of Israel*, 1987).

3.2. SIGNIFICANT CHANGES OF METEOROLOGICAL VARIABLES IN THE SOUTH DEAD SEA

Meteorological data at Sdom (S) from recent years was compared to those measured previously by Ashbel (1975). The measuring station at S remained at nearly the same location during these years. Three different climate stations operated in the 1930s–1940s; in 1934, measurements were at the foot of the Salt mountain; in 1936, at the evaporation ponds (S) and in 1942, near the Dead Sea Works Factory. Ashbel used the 1936 (evaporation pond) station and the present S measurements are also at the evaporation ponds. The station that operated in 1942 is the one currently maintained by the Israel Meteorological Service.

Over 45,000 observations were considered for the relative humidity calculation in the 1935–1941 period, and over 20,000 observations in the 1985–1987 period. For the temperature calculations the corresponding numbers are over 35,000 and over 15,000. The same calculating procedure was applied in all cases. First, the monthly average from the hourly means was calculated, than the annual average. All available data were considered for the calculations. The average humidity in the 1937–1942 period* was 55%, as compared to 46% in the recent 1985–1987 period (Issahary et al., 1985, 1986, 1987). This 9% decline implies an evaporation increase. The average temperature from Ashbel's data (1975) was 25.7 °C while the present temperature is 26.3 °C. This 0.6 °C increase also implies an increase in pan evaporation.

In order to statistically examine the more recent changes, hourly meteorological data at Sdom between 1975–1989 were studied. The meteorological parameters examined were air dry and wet-bulb temperatures, wind speed, cloud amount and pan evaporation. Based on the T-test the significance of the changes in these hourly parameters was determined by comparing the recent period of 1982–1989 with the 1975–1981 period before pan evaporation increased.

The calculation procedure was as follows. The hourly data at 08, 14 and 20 for each month, year and parameter were employed to calculate monthly averages for each hour. Then, the means for the first period (1975–1981) and the second (1982–1989) were computed. The statistical tests' results are presented in Table I. The main conclusions were that wind speeds from March to July have statistically decreased; air temperatures from February to June have decreased, but increased for July

to September. The wet-bulb temperatures show a similar trend to that of the dry bulb temperatures. Finally, evaporation increased from April to September (see also Figure 4).

* Ashbel (1975) used for humidity measurements the classical hair hygrograph while recent measurements were taken by the same method during 1985–1986 and in 1987 through the dry and wet-bulb temperatures, Issahary (1987). Although the instrumental changes are large, these changes are statistically significant higher than 99% and are in the same direction as our other findings to be presented next.

Table I

Significant changes of average hourly meteorological parameters at Sdom. New period (1982–1989) against previous period (1975–1981). First line: + increase, – decrease of parameter in last period. Second line: The difference of parameter between two periods. Third line: The significant level of the climatic change – three stars (∗ ∗ ∗): Significant level of more than 99%, two stars (∗∗) – more than 97.5%, one star (∗) – more than 95%, without star – more than 90%. A blank box denotes insignificant change

Param.	Month / Hour	Jan	Feb	Mar	Apr	May	Jun	Jul	Aug	Sep	Oct	Nov	Dec
Temperature (°C)	08	+ 0.9 ***		– 0.5				+ 0.3	+ 0.6 ***	+ 0.8 ***	+ 0.4		
	14	– 0.6 * *	– 1.0 ***	– 1.4 ***	– 0.7 * *	– 1.2 ***	– 0.5	– 0.4 *	+ 0.5 ***	+ 0.6 ***			– 0.5 *
	20		– 0.8 ***	– 0.8 * *				+ 0.7 ***	+ 1.0 ***	+ 0.7 ***			
Wet-Bulb Temperature (°C)	08	+ 0.6 ***				– 0.4 ***	– 0.3 *	+ 0.4 * *	+ 0.6 ***	+ 0.6 ***		+ 0.5	
	14	– 0.4 * *	– 0.8 ***	– 0.5 * *	– 0.5 ***	– 0.8 ***	– 0.6 ***			+ 0.2	– 0.4		– 0.4 *
	20		– 0.6 ***	– 0.4 *		– 0.6 ***	– 0.3 *	+ 0.4 ***		+ 0.3 *		+ 0.4	
Wind Speed (m/s)	08	+ 1.3 *		– 1.2	– 1.6 * *	– 1.0	– 0.9 *	– 1.3 ***	– 0.5				
	14			– 1.8 ***	– 1.2	– 2.2 ***		– 1.2 ***	– 0.5				
	20			– 2.2 ***		– 1.8 * *	– 2.1 ***				+ 1.0		
Cloud Amounts (eighth)	08			+ 1.0 ***					– 0.3 *	– 0.2			
	14			+ 0.7 * *	– 0.5 *			– 0.2 ***		– 0.3 *		+ 0.6 *	
	20	+ 0.6 * *	+ 0.7 * *	+ 0.7 ***			+ 0.1					+ 0.8 ***	+ 0.4
Evap. (mm)	Daily	+ 0.5 ***	+ 0.3	– 0.4	+ 0.6 *	+ 1.0 ***	+ 1.5 ***	+ 1.1 ***	+ 1.2 ***	+ 1.3 ***		+ 0.7 * *	

We have also examined with the same procedures the climatic trends in other stations of the Jordan Valley. i.e., Tirat Zvi, Jericho and Eilat, Figure 1. Table II summarizes the significance of changes in the monthly averages of relative humidity, temperature, wind speed, atmospheric pressure and cloud amounts between the recent period (1982–1990) compared with the earlier one (1966–1981). The periods averaged are not exactly corresponding to those of pan evaporation because of data availability. In contrast to the calculations from Sdom in Table I, where hourly data were used, in Table II derivations of the monthly mean data were employed and a similar pattern to that found at Sdom in Table I was obtained. At Sdom (S), a reduction in the May–July wind speed was found; an increase in July–September temperature and a decrease in the relative humidity in May–June. These changes were not found at the other three Jordan Valley stations. On the contrary, an increase in wind speed was found at Jericho and Eilat, and an increase of relative humidity in Tirat Zvi and Jericho. It should be noted that in other months there is also an increase in temperature and decrease in relative humidity at Sdom but these are not statistically significant. Another finding was increases in air pressure at Jericho and Eilat for several months. Also, the seemingly highly significant decrease in wind speed at Tirat Zvi is certainly an instrumental error (J. Mishaelli, pers. comm.). A hypothesis to explain these changes is presented next.

3.3. EXPLANATION TO THE INCREASE IN PAN EVAPORATION AT THE SOUTH DEAD SEA

As a result of its decreasing area the Dead Sea breeze has weakened. This wind normally moderates the Dead Sea climate, and its weakening causes a decrease in relative humidity, and an increase in the air temperature, and consequently pan evaporation to increase. These climatic changes are most marked during the Spring–early Summer months when the sea-land temperature differences are at their maximum since the lake is still cold from the low winter temperatures, while the land has already warmed. Therefore, during these months a climatic change toward a hotter and drier climate is expected as well as an increase in the pan evaporation.

4. Role of the Dead Sea Breeze in Tempering the Climate of the Dead Sea Region

4.1. THE DEAD SEA BREEZE AND ITS INFLUENCE ON TEMPERATURE

Figure 6a shows the diurnal variation for the normalized February–June mean wind speed at Sdom (S), during the recent period of 1987–1989 (measured by D. Issahary), and the past period of 1935–1941 (Ashbel, 1975). There are differences in the *absolute* wind speed between the two curves probably due to the instrumentation. Ashbel (1975) analysed measurements using a Dines anemograph that

Table II

Significant changes of average monthly meteorological parameters in four stations at the Jordan Valley. New period (1982–1990) against previous period (1966–1981). RH – means Relative Humidity, T – Temperature, V – Wind Speed, P – Atmospheric Pressure and C – Cloud Amounts. First line: + increase, – decrease of parameter in last period. Second line: The difference of parameter between two periods. Third line: The significant level of the climatic change as in Table I. The single # signs missing data, while ## signs data error

Sta	Month	Jan	Feb	Mar	Apr	May	Jun	Jul	Aug	Sep	Oct	Nov	Dec
	Param.												
Tirat Zvi	RH (%)						+ 1.3 *	+ 1.7 *	+ 1.4 *			+ 5.6 * *	
	T (°C)								+ 0.4	+ 0.4	− 0.7 *	− 1.0	
	V (m/s)	# #	# #	# #	# #	# #	# #	# #	# #	# #	# #	# #	# #
	P (hPa)	#	#	#	#	#	#	#	#	#	#	#	#
	C eighth										+ 2.6 *	+ 3.8 *	
Jericho	RH (%)												
	T (°C)										− 0.6		
	V (m/s)		+ 0.8 *	+ 0.7 *			+ 1.0 *	+ 1.1 *		+ 0.9 *	+ 0.7 *		
	P (hPa)	+ 1.7 *	+ 1.5 *		+ 1.2 *	+ 1.0 * * *	+ 1.3 * * *	+ 0.8 *			+ 0.8 *		
	C eighth				− 0.8 * *		− 0.3 * * *	− 0.3 * * *	− 0.3 * * *	− 0.3 * * *			
Sdom	RH (%)		− 2.8 * *			− 3.4 * *	− 3.5 *						
	T (°C)							+ 0.9 * * *	+ 0.7 * *	+ 0.4 *			
	V (m/s)					− 1.1 * * *	− 1.9 * * *	− 1.9 * * *		− 1.2 *			
	P (hPa)	#	#	#	#	#	#	#	#	#	#	#	#
	C eighth									− 0.2 *			
Eilat	RH (%)		− 2.2										
	T (°C)			− 0.7 *						+ 0.5 *	− 0.8 *		
	V (m/s)	+ 1.4 * *		+ 0.9 *	+ 0.8 *	+ 1.1				− 0.8		+ 0.7	+ 1.4 * * *
	P (hPa)	+ 1.9 * * *	+ 1.2 *	+ 1.1	+ 0.8	+ 1.0 * * *	+ 1.2 * * *	+ 0.8	+ 0.7		+ 1.0 * * *	+ 0.8	+ 1.1 * *
	C eighth				− 0.7 * *		− 0.2 * *						

suffered from strong corrosion in the climate of the Dead Sea, Ashbel (1975), while recent measurements are based on cup anemometers. Therefore, Figure 6a presents the normalized wind speed at the two periods performed by subtracting the daily means and dividing by the standard deviations in each of the two periods, respectively. Figure 6a suggests a climatic change in the local diurnal pattern of the lake breezes. During the two periods the wind speed increase from the morning till noon time is characteristic of the breeze (Alpert et al., 1982). In the earlier period, however, the wind speed began to rise as early as 7 a.m., intensified at 9 a.m., and reached its peak at 3 p.m. while more recently, the wind speed rise begins only at around 10 a.m. and reaches its peak later at 4 p.m.. Hence, the diurnal wind speed amplitude which reflects the local sea breeze was much emphasized during the 1930s–1940s compared to recent data. Also, in the recent wind speed variations another maximum at 8 p.m. exists. This maximum is not found in the 1935–1941 averages and will be explained in the next section.

Figure 6b shows the air temperature at the Southern Dead Sea. The temperature in the 1930s–1940s in the morning hours was somewhat lower than today and the maximum daily temperature occurred one hour later. A possible change in the recording time may be ruled out, since the phase changes in Figure 6a, b are *not* in the same direction. The phase shift and the higher recent maximum can be explained by the weakening and delaying of the lake breeze. In the past, this local breeze cooled the air and moderated the temperature rise during the morning hours. Now, this effect is weaker, and a steep temperature rise occurs in the morning and the temperature peaks earlier. It should be noted that each hourly data in Figure 6a, b is the mean of about 600 measurements in the 1930–1940, and about 450 measurements in the 1980–1990. However, given the short time series, particularly for the wind (Figure 6a), and the instrument changes, these findings should be treated with some caution.

4.2. SPECIAL OBSERVATIONAL PERIOD AT THE DEAD SEA

To further investigate the role of the Dead Sea breeze in affecting the local climate, special observations were conducted at the Dead Sea western coast during the 10–13 May 1992, a season when the breeze is particularly strong. The wind vector, temperature, wet-bulb temperature, radiation and pan evaporation were measured simultaneously at six automatic stations whose locations are indicated in Figure 7. Measurements at stations KR and S were made every minute and averaged every hour, while at stations RR and CR measurements were made every 20 s and averaged every 10 min. For stations JR and J only the 08, 14 and 20 measurements were available. Figure 7 is for noon (2 p.m.) of 12 May and for evening (8 p.m.) of the 10 May (dashed). At noon, the wind direction is north-westerly in Jerusalem, and north-easterly in Jericho. However, the wind direction in the Dead Sea stations is from the Lake. In KR, RR, CR and S winds blow with a local lake breeze component. These effects were also noted by Bitan (1977).

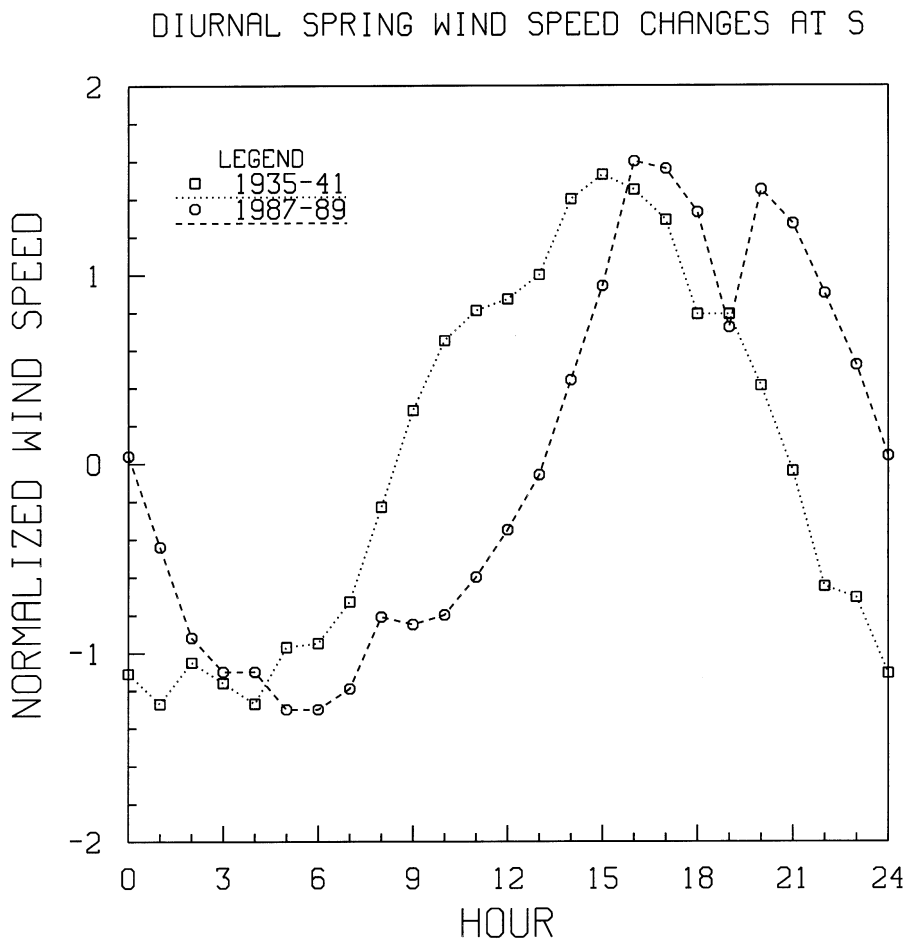

Figure 6a.

At the evening of 10 May another phenomenon characteristic for the Dead Sea climate was noticed. At this time, the Mediterranean breeze reaches the Dead Sea in the Spring and Summer. The airmass associated with this wind falls about 1200 m from the Judean Mountains, heats adiabatically, dries and penetrates the Dead Sea region. A similar phenomenon further north at the Sea of Galilee was also simulated and discussed by Alpert et al. (1982). The wind directions in the evening are westerly to north-westerly with relatively high speeds of 5–10 knots at all the stations (Figure 7, dashed). The hot and dry wind certainly affects the evaporation in Sdom. The adiabatic heating and drying of the Dead Sea region increases the evaporation (Ashbel, 1939). Hence, the changes in the interaction of the Mediterranean breeze with the Dead Sea breeze in the presence of the steep topography may have therefore caused the increase in pan evaporation at Sdom in recent years. In the past, when the Dead Sea breeze was stronger, it delayed

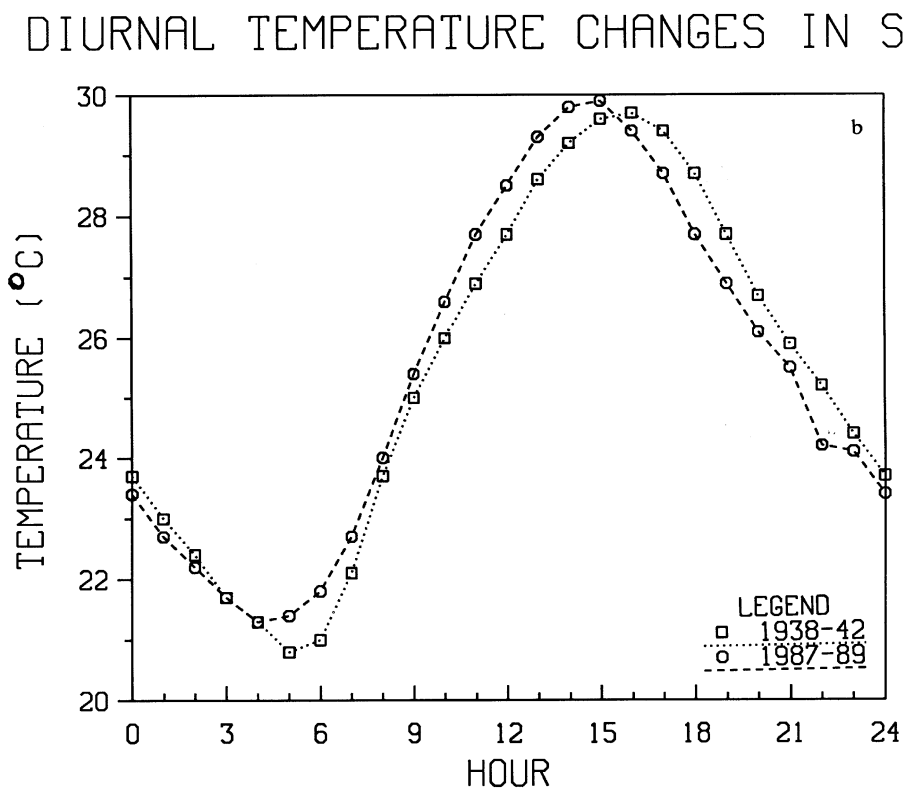

Figure 6b.

Figure 6. Diurnal variations in (a) normalized wind speed, (b) temperature at Sdom for the February–June means. New 1987–1989 and older 1935–1941 periods, are shown.

the penetration of the Mediterranean breeze. Due to the recent weakening of the Dead Sea breeze, the Mediterranean breeze penetrates strongly into the Dead Sea region, and this hot and dry wind increases the evaporation. This happens during both Spring and Summer when the Mediterranean breeze is significant. The phenomenon is clearly seen in Figure 6a. A new peak in the wind speed is observed in the more recent years at 8 p.m., while in the past, when the Dead-Sea breeze delayed the Mediterranean breeze penetration, this peak is missing.

Figure 8 shows the diurnal temperature on the 12 May 1992. From 8 a.m. till 3 p.m. the highest temperature was measured in Sdom, and the lower temperature was recorded on RR with medium values at CR. S is the farthest from the lake of these stations, while RR is the closest. As suggested earlier, this temperature characteristic is strongly related to the lake breeze, which cools the areas neighboring the Northern basin but is weaker further to the south. In the next section our hypothesis will be examined with the aid of mesoscale model simulations.

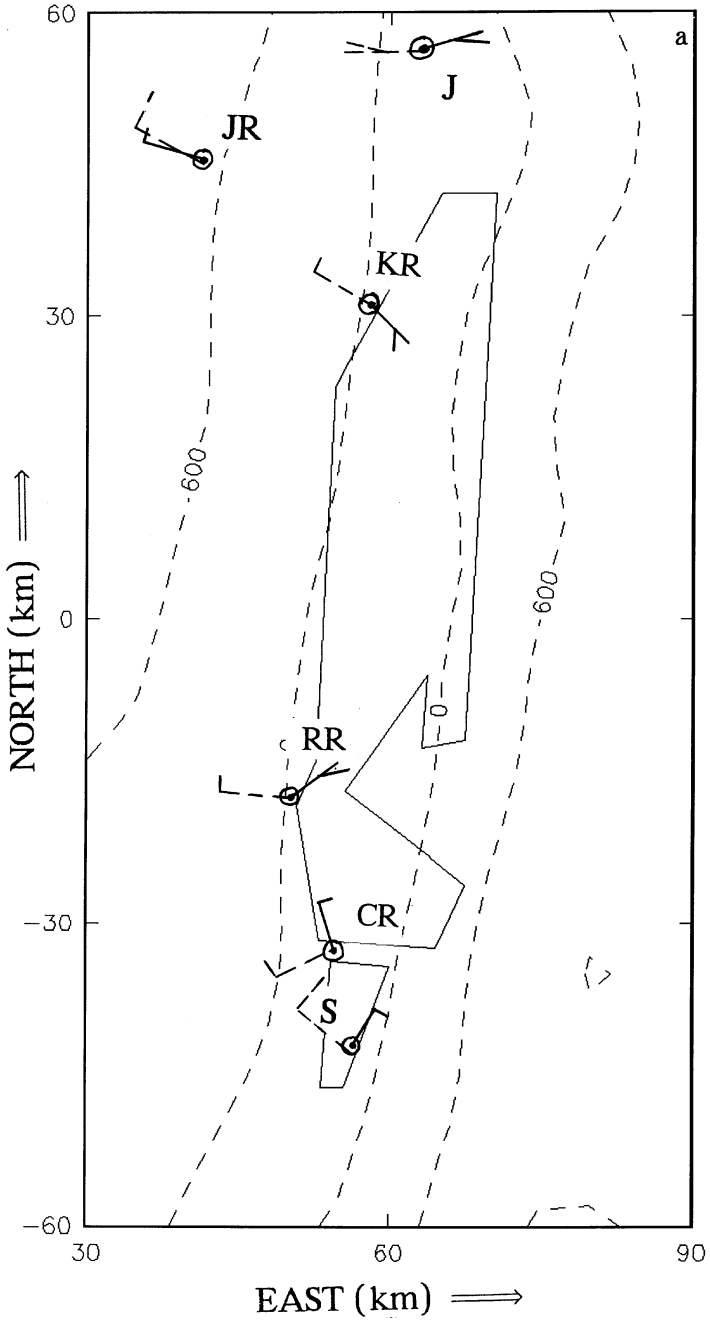

Figure 7. Surface wind vectors for 12 May 1992 12 UTC (solid) and for 10 May 18 UTC (dashed). Arrows indicate wind direction, and line on top of the arrow its speed: diagonal line – 3 knots, short line – 5 knots, long line – 10 knots. Open circles denote fair weather. Letters JR, J, KR, RR, CR and S stand for Jerusalem, Jericho, Kidron River, Rachaf River, Chemar River and Sdom, respectively.

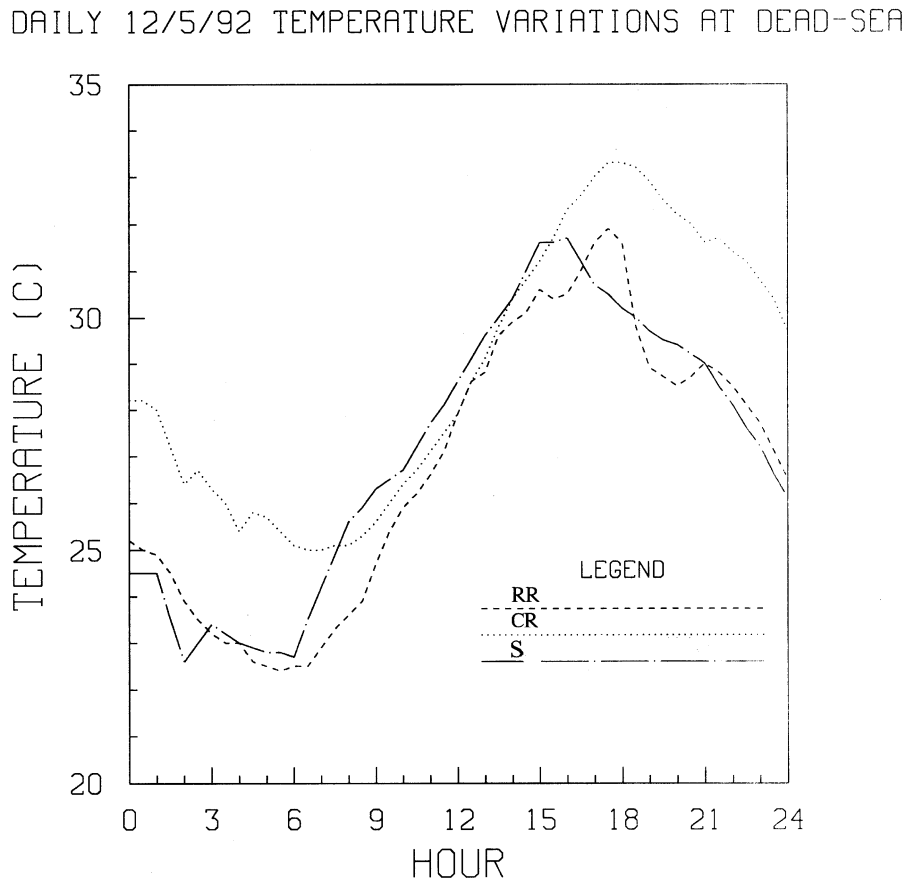

Figure 8. Diurnal temperature variations at RR, CR and S on 12 May 1992.

5. Mesoscale Modeling

5.1. THE MODEL AND BACKGROUND DETAILS

A three-dimensional model was run in order to investigate the proposed hypothesis for the climatic change in the Dead Sea region. The NCAR/PSU model version MM4 (Anthes et al., 1987) was run for 24 h for a late Spring-early Summer event on 17 June, 1987, at time when a very pronounced local change was noticed. For the surface-evaporation fluxes calculations the model uses the explicit, high resolution PBL model (Zhang and Anthes, 1982) and the fluxes formulation follows Carlson and Boland (1978). The model domain was 360 $\times$ 360 km; grid size of 5 km, and with 16 vertical levels at the altitudes of 1000 hPa, 991, 982, 964, 937, 901, 856, 802, 730, 640, 550, 460, 370, 280, 190 and 100 hPa. A time step of 10 sec was used and for the initialization six soundings from the area were employed (Figure 1). This initialization and other aspects of our high-resolution mesoscale simulations

Table III
Description of land-use categories and physical parameters used in the 3-D model simulations

No.	Land-use description	Albedo (%)	Moisture avail. (%)	Emissivity (% at 9 μm)	Roughness length (cm)	Thermal inertia (cal cm^{-2} K^{-1} s$^{-0.5}$)
1	Water	8	100	98	0.0001	0.06
2	Wet land	14	50	95	20	0.06
3	Desert	25	2	85	10	0.02

over the region can be found in Lieman and Alpert (1993). Since the evaporation of the Dead Sea water is about half that of pure water (Stanhill, 1994), moisture availability for the Dead Sea grid points was assumed 0.5. Over the Dead Sea, 47 points exist in the model domain, 34 of which over the Northern basin and 13 over the Southern basin. The latter includes the evaporation ponds of the Dead Sea Works. Three runs were performed; the first run with the Dead Sea area as it was before 1979. In the second run the Dead Sea was omitted, and all its grid points are in the state of a 'desert'. The third run represented the Dead Sea at its present configuration. In the latter, the Northern basin exists as a full sea (neglecting the decrease in its area as well), and the Southern basin is partly dry in the following manner. Two grid points west to the Lisan Straits are dry land – 'desert', and the rest assumed 'wet land'. This reflects the state of the Dead Sea in the last decade, in which part of the Southern basin is dry, and the other part exists artificially. The second part is represented by 'wet land' of the land use category although the physical characteristics of the ponds are somewhat different than the 'wet land'. For the different categories of land-use parameters used in the model for the Summer see Table III (from Anthes et al.,

1987). The roughness length may not fit well into these land-use but these effects were neglected. Also, the Dead Sea water temperature was assumed constant at 30 °C, the mean June value (Ashbel, 1975) ignoring the daily variation of about 5 °C (Ashbel, 1975). However, over the Southern Dead Sea 'wet-land' grid points in the model were allowed to change the 'water' temperatures. The Mediterranean sea surface temperature was assumed constant at 23.5 °C. Other important effects ignored in the present runs are the effect of the increase of the Dead Sea SST in the last 50 years as reported by Stanhill (1990), and the reduction of the global irradiance at Sdom as reported by Cohen and Stanhill (1996). Here the focus was solely to estimate the potential contribution of the changing area of the Dead Sea.

5.2. SIMULATED CHANGES OF THE DIURNAL METEOROLOGICAL FIELDS AT THE SOUTH DEAD SEA

Simulated diurnal variations of wind speed (a), temperature (b), relative humidity (c) and pan evaporation (d) on 17 June 1987 at Sdom for the three runs are shown in Figure 9a–d. The three runs were as follows. First, the 'full sea' – the Dead Sea

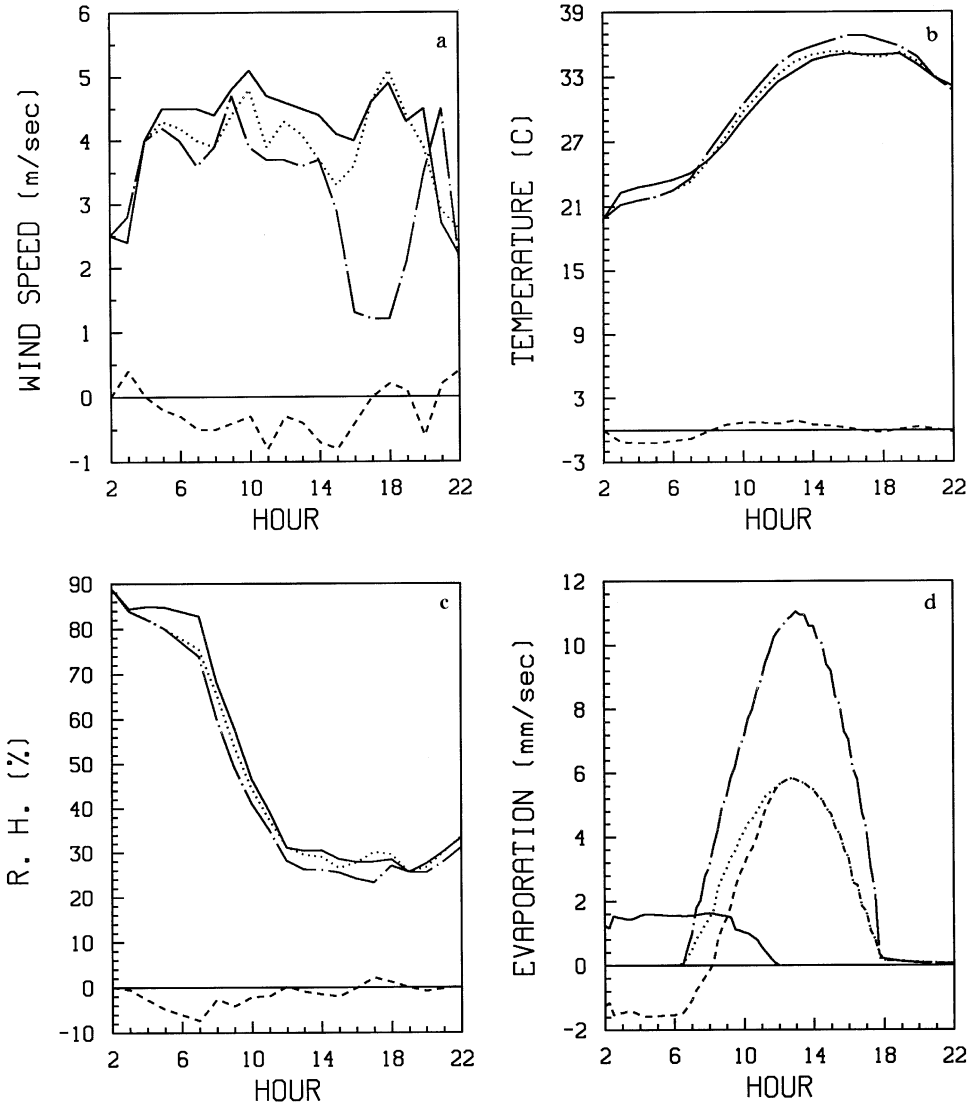

Figure 9. Model simulated diurnal changes in the meteorological fields at Sdom on 17 June 1987. The 'full sea' run – full line; 'no sea' – dashed-dotted line; 'present sea' – dotted line; difference fields, i.e., 'full sea' minus 'present sea' – dashed line at the bottom. (a) wind speed (m s^{-1}), (b) temperature (°C), (c) relative humidity (%), (d) pan evaporation flux (mm $s^{-1} \times 10^{-4}$).

as it used to be in the past, the 'present sea' – present state of the sea and 'no sea'. At the bottom of each figure the differences between 'present sea' and 'full sea' are shown. These differences represent the model simulated climatic changes induced by the area shrinking of the Dead Sea.

The wind speed, depicted in Figure 9a, shows two peaks, at 10 a.m. and at 4 p.m. The first peak is related to the Dead Sea sea-breeze, while the second refers to the

penetration of the Mediterranean Sea breeze. The strongest daily wind speed is for the 'full sea' run, while the lowest speed is for the 'no sea' run. The 'present sea' run shows the intermediate values. The wind direction during the day is easterly, reflecting the local lake breeze. It is missing when the sea is absent and partly exists in the present state of the sea. The mean sea breeze is 4–5 m s^{-1} for the 'full sea' run, 3.5–4.5 m s^{-1} for the 'present sea' and 3–4 m s^{-1} for 'no sea'. The weakening of the breeze is shown at the base of the figure. The difference in wind speed between 'full sea' and 'present sea' is up to 0.8 m s^{-1} at 11 a.m. and at 3 p.m. At 4 p.m. the Mediterranean breeze penetrates the region, and the wind speed reaches 5 m s^{-1} with a north-westerly direction.

As expected, the daily temperature is highest in the 'no sea' run (Figure 9b). With 'full sea' the temperature is lowest, and again the 'present sea' has intermediate values. During the night the picture is opposite and the 'full sea' state has maximum values. The temperature reached its peak at 4 p.m., 36.8 °C without the sea, 35.1 °C for the 'full sea' and 35.3 °C for the present sea. The Dead Sea clearly tempers the temperature in its vicinity. During the day it lowers and during night it raises the neighborhood's temperature, see the difference line. The difference reaches a maximum of 0.9 °C at 1 p.m.

The relative humidity (Figure 9c), is high during the night and low during the daytime because of its reversed relationship with the temperature. The relative humidity is highest for 'full sea', lowest for 'no sea', and has intermediate values for 'present sea'. The influence of the sea on the relative humidity of its neighboring areas is twofold; first, a water source increases the relative humidity in its vicinity, and secondly, the cooling of the air causes an increase in relative humidity. In the present state of the sea, the relative humidity is less than in the past because of the sea's drying. The difference between the runs reaches 7% at 7 a.m., with the negative difference noticed throughout the day.

Figure 9d shows the calculated pan evaporation based on the model simulations, i.e. assuming moisture availability of 1 or doubling the model results calculated for moisture availability of 0.5. The maximum pan evaporation is for 'no sea', while the evaporation is minimal for 'full sea'. The difference between the past and present state runs reaches a value of 5.5×10^{-4} mm s^{-1} at noon. The total daily pan evaporations at the three runs were computed as follows. First, the mean evaporation fluxes of the day were found. Next, the daily evaporations were found and multiplied by the ratio between the moisture availability of pure water (100%), and that of the grid point under investigation in every run. Hence, the total daily pan evaporations at S was found to be 5.9 mm d^{-1} for 'full sea', 27.4 mm d^{-1} for 'no sea' and 14.4 mm d^{-1} for the 'present state'. These estimates may be compared with the actual value of 18.5 mm d^{-1} measured on 17 June 1987. It should be noted that the model seems to predict quite high values for the 'no sea' case as compared to the Jordan Valley values, but this may be due to the even drier conditions over the hypothetically totally dry Dead Sea.

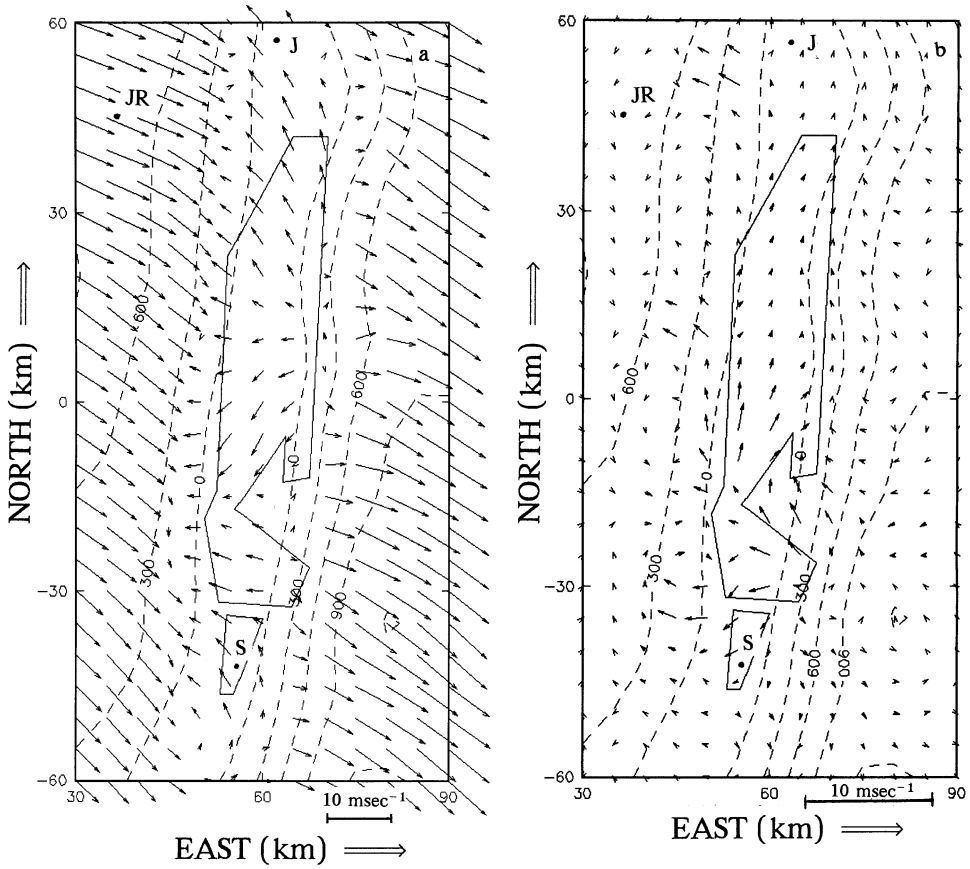

Figure 10. Model-simulated surface winds (m s^{-1}) on 17 June 1987 12 UTC (14 LT). Scale of the wind speed is at the bottom. Topography is dashed with 300 m interval. Letters JR, J and S stand for Jerusalem, Jericho and Sdom
respectively. (a) 'present sea' (b) the difference, i.e. 'full sea' minus 'present sea'.

5.3. AREAL DISTRIBUTIONS OF THE METEOROLOGICAL FIELDS

Figures 10–13 show the geographical distributions of the wind vector, temperature, relative humidity and lake evaporation respectively at 12 UTC (1400 LST or 1500 with Summer time). In each of the figures (a) is for the present state, and (b) is the difference map between 'present state' and 'full sea' ('full sea' minus 'present sea'). Hence, (b) represents the simulated climatic change.

Figure 10a, b shows the wind vectors. The Mediterranean breeze does not penetrate the Dead Sea region at noon, while close to the Dead Sea the easterly lake breeze dominates (Figure 10a). From the difference map (Figure 10b) ('full sea' minus 'present sea') the influence of the Dead Sea drying on the local breeze can be seen. The difference is especially apparent in the Southern basin where the change

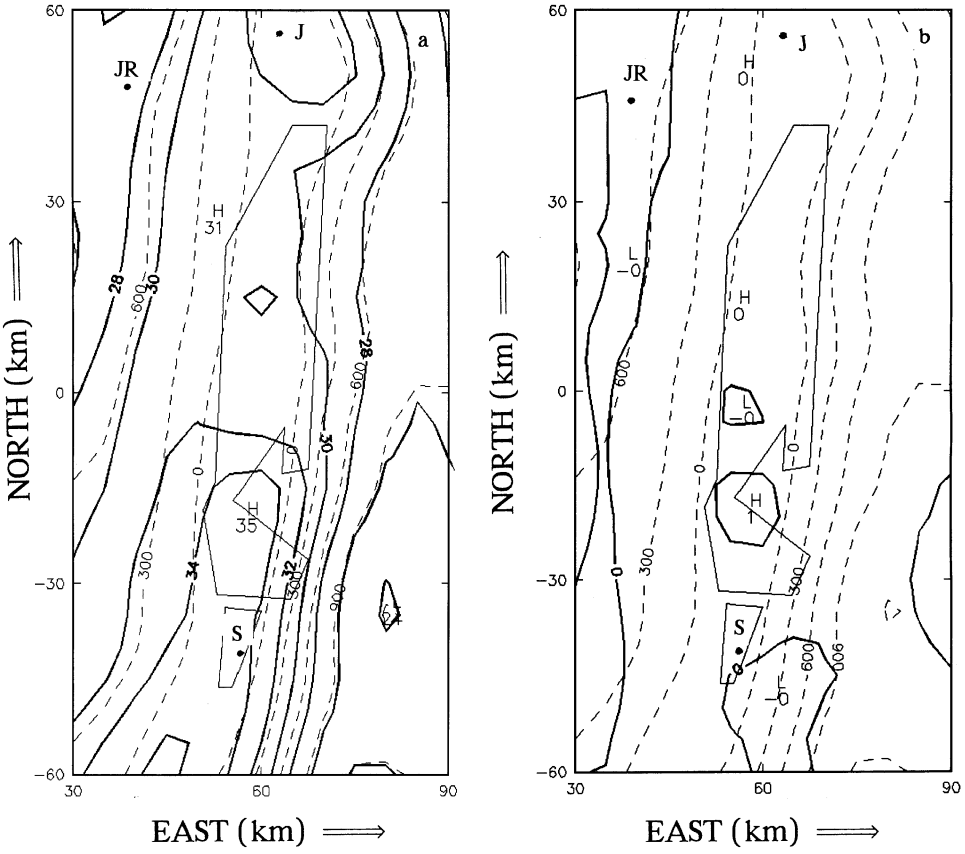

Figure 11. As Figure 10 but for the surface temperature (°C). Here, the difference is 'present sea' minus 'full sea'. Temperature interval is 2 °C in (a) and 1 °C in (b).

in land-use took place. The difference wind vectors in the Southern basin represent the weakening of the Dead Sea breeze.

Figure 11a, b is for air temperatures at 12 UTC. The difference map ('present sea' minus 'full sea' in this case) shows a difference of 1 °C in the Southern basin, representing the simulated climatic change in temperature.

Figure 12a, b is for relative humidity. A high value of 45% over the lake is noticed in Figure 12a, compared to 20–25% over the land. Figure 12b shows

a difference of –4% between the two runs, representing the simulated effect of the climatic change on the relative humidity.

Figure 13a, b presents the lake evaporation maps. As already mentioned, the salinity effect of the Dead Sea was taken into account by reducing the moisture availability to 0.5. A high value of evaporation flux of 13.5×10^{-5} mm s^{-1} for the Southern basin can be seen in Figure 13a. The increase in lake evaporation reaches

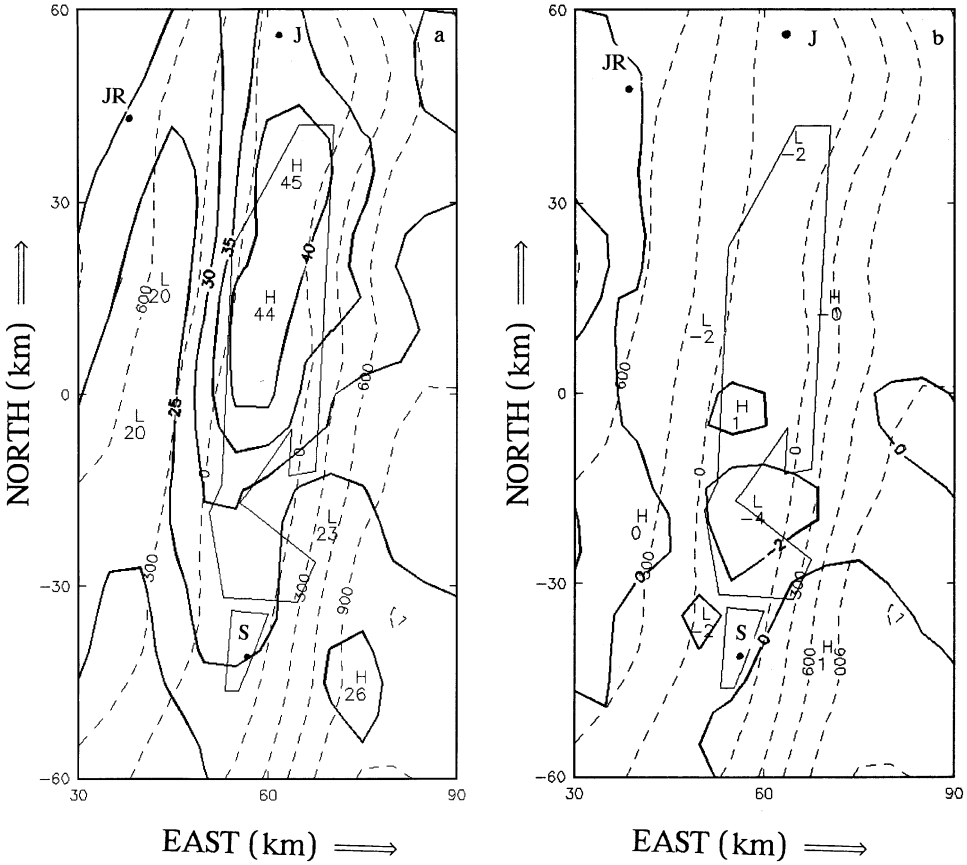

Figure 12. As Figure 11 but for the relative humidity (%). The interval is 5% in (a) and 2% in (b).

a value of 10×10^{-5} mm s^{-1} at noon over the Southern basin, with a 7×10^{-5} mm s^{-1} increase in S (Figure 13b).

6. Discussion

Morton (1983) suggested a similar hypothesis to the one adopted here. Based on his model results, he proposed that an inverse relationship exists between actual (areal) and potential (pan) evaporation. He has explained this by a micro-climate modification. Two main processes seem to act while the Dead Sea dries. Both processes tend to increase the potential evaporation. The first process was described in this study and similarly in Morton (1983). In our study, it is the modification of the micro-climate through dynamical changes in the Mesoscale circulations. The weakening of the local sea-land breeze causes an increase in air temperature, a decrease in relative humidity, and thus, an increase in the pan evaporation.

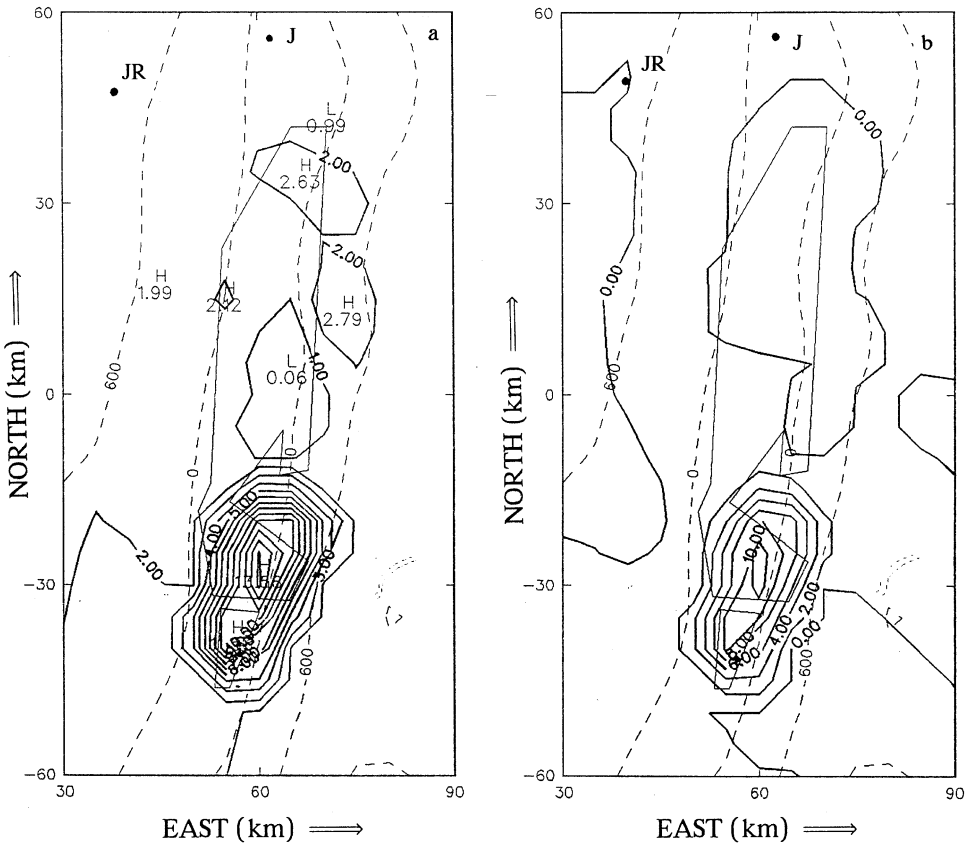

Figure 13. As Figure 11 but for the lake evaporation (mm $s^{-1} \times 10^{-5}$). Evaporation flux interval is 1×10^{-5} mm s^{-1} in (a) and 2×10^{-5} mm s^{-1} in (b).

The second process is the increase in salinity of the lake. Stanhill (1994) suggested that decrease in the evaporation from the Dead Sea was accompanied by the increased salinity from the Sea. Obviously, the reduction of the Dead Sea area was associated with increased salinity. The reduced evaporation from the Sea diminishes the relative humidity in the air, which in turn may further *increase* the pan evaporation at the Southern Dead Sea. It will be helpful to run the model with the salinity changes as well. It can be done by reducing in the model, the Sea moisture availability at the Southern Dead Sea. Further research on the salinity variations potential effect on the climatic change is beyond the scope of this preliminary study.

7. Summary

Three-dimensional model simulations in combination with measurements and statistical calculations strongly suggest that a climate change has occurred at the Southern basin of the Dead Sea. The evidence presented here associates the Dead Sea breeze weakening with the drying of the Dead Sea and reduction in its area. The breeze, which tempers the climate of the Dead Sea, becomes less vigorous, especially in the Spring early-Summer months when it probably causes increases in the air temperature and decreases in the relative humidity, causing an increase in the pan evaporation at the South Dead Sea. This hypothesis indicates a desertification tendency in the Dead Sea climate.

Acknowledgements

This work was partly performed while the first author (PA) held a National Research Council – NASA/GSFC Research Associateship. We wish to express our gratitude to Marina Tsidulko, Ronen Liman and Yuval Shay-El for their assistance in running the 3-D model and drawing the maps. Thanks to Dr. Ayal Anis for his helpful comments, and to the Israel Meteorological Service for parts of the data. We thank also Dr. Noah Wolfson and Dr. Zipora Klein for their helpful comments, and Dr. Alex Manes and Prof. G. Stanhill for their help in obtaining Dead Sea data. Thanks to Dr. Anati for data of the Dead sea MSL changes. We thank the reviewers for their very helpful comments and particularly to Rev. A for his extensive and most valuable comments.

References

Alpert, P., Cohen, A., Neumann, J., and Doron, E.: 1982, 'A Model Simulation of the Summer Circulation from the Eastern Mediterranean past Lake Kinneret in the Jordan Valley', *Mon. Wea. Rev.* **100**, 994–1006.

Anati, D. A.: 1997, 'Hydrography of a Hypersaline Lake', *The Dead Sea*, Oxford University Press, Oxford, in press.

Anati, D. A. and Shasha, S.: 1989, 'Dead Sea Surface Level Changes', *Isr. J. Earth Sci.* **38**, 29–32.

Anati, D. A., Stiller, M., Shasha, S., and Gat, J. R.: 1987, 'Changes in the Thermo-Haline Structure of the Dead Sea: 1979–1984', *Earth Planet. Sci. Lett.* **84**, 109–121.

Anthes, R. A., Hsie, E. Y. and Kuo, Y. H.: 1987, 'Description of the PSU/NCAR Mesoscale Model Version 4 (MM4)', NCAR Tech. Note 282-STR, p. 66.

Ashbel, D.: 1939, 'The Influence of the Dead Sea on the Climate of Its Neighborhood', *Quart. J. Roy. Met. Soc.* **115**, 185–194.

Ashbel, D.: 1975, 'Forty Five Years of Observations in the Climate and Hydrology of the Dead Sea', The Hebrew Univ. of Jerusalem, p. 183 (in Hebrew).

Bitan, A.: 1974, 'The Wind Regime in the North-West Section of the Dead Sea', *Arch. Met. Geophys. Bioklim.* **22** (Ser. B), 313–335.

Bitan, A.: 1977, 'The Influence of the Special Shape of the Dead Sea and Its Environment on the Local Wind System', *Arch. Met. Geophys. Bioklim.* **24** (Ser. B), 283–301.

Carlson, T. N. and Boland, F. E.: 1978, 'Analysis of Urban-Rural Canopy Using a Surface Heat Flux/Temperature Model', *J. Appl. Meteor.* **17**, 998–1013.
Cohen, S. and Stanhill, G.: 1996, 'Contemporary Climate Change in the Jordan Valley', *J. Appl. Meteor.* **35**, 1051–1058.
Hydrological Year Book of Israel: 1987, Ministry of Agriculture, Water Commission, Hydrological Service.
Israel Meteorological Service: 1967, *Standard Climatic Average of Rainfall Amounts 1931–1960*, Ser. A, Meteorological notes no. 21, Israel Meteorological Service, Bet Dagan 50250, Israel (in Hebrew).
Issahary, D., Maymon, M., and Sadik, Z.: 1985, *Yearly Meteorological Summary, 1985*, Dead Sea Works, Sdom, p. 41.
Issahary, D., Maymon, M., and Sadik, Z.: 1986, *Yearly Meteorological Summary, 1986*, Dead Sea Works, Sdom, p. 55.
Issahary, D., Sadik, Z., and Maymon, M.: 1987, *Yearly Meteorological Measurements Summary, 1987*, Dead Sea Works, Sdom, p. 48.
Klein, C.: 1982, 'Morphological Evidence of Lake Level Changes, Western Shore of the Dead Sea', *Isr. J. Earth Sci.* **31**, 67–94.
Klein, C.: 1985, *Dead Sea Entree, Israel Atlas* (3rd ed.), Naphtaly Kadmon (ed.), Measurement Dept., Tel Aviv, Carta, Jerusalem, p. 119.
Lieman, R. and Alpert, P.: 1993, 'Investigation of the Planetary Boundary Layer Height Variations over Complex Terrain', *Bound. Layer Meteor.* **62**, 129–142.
Mass, C. F. and Portman, D. A.: 1989, 'Major Volcanic Eruptions and Climate: A Critical Evaluation', *J. Climate* **2**, 566–593.
Morton, F. I.: 1983, 'Operational Estimates of Lake Evaporation', *J. Hydro.* **66**, 77–100.
Oren, A.: 1993, 'The Dead Sea – Alive Again', *Experientia* **49**, 518–522.
Song, N., Starr, D. O'c., Wuebbles, D. J., Williams, A., and Larson, S. M.: 1996, 'Volcanic Aerosols and Interannual Variation of High Clouds', *Geophys. Res. Lett.* **23**, 2657–2660.
Stanhill, G.: 1990, 'Changes in the Surface Temperature of the Dead Sea and Its Heat Storage', *Int. J. Climatol.* **10**, 519–536.
Stanhill, G.: 1994, 'Changes in the Rate of Evaporation from the Dead Sea', *Int. J. Climatol.* **14**, 465–471.
Steinhorn, I.: 1981, 'A Hydro-Graphical and Physical Study of the Dead Sea during the Destruction of Its Long-Term Meromictic Stratification', Ph.D. Thesis, Weizmann Institute of Science, Rehovot, p. 323.
Zhang, D. L. and Anthes, R. A.: 1982, 'A High Resolution Model of the Planetary Boundary Layer – Sensitivity Tests and Comparison with SESAME – 79 Data', *J. Appl. Meteorol.* **21**, 1594–1609.

(Received 24 April 1995; in revised form 23 January 1997)